Published in final edited form as:
J Theor Biol. 2009 May 7; 258(1): 112–120. doi:10.1016/j.jtbi.2008.12.021.

Inheritance of epigenetic chromatin silencing

Diana David-Rus[a,*,1], **Swagatam Mukhopadhyay**[a,b,1], **Joel L. Lebowitz**[b,c], and **Anirvan M. Sengupta**[a,b,*]

Diana David-Rus: ddavid@rci.rutgers.edu; Swagatam Mukhopadhyay: swagatam@rci.rutgers.edu; Joel L. Lebowitz: lebowitz@math.rutgers.edu; Anirvan M. Sengupta: anirvans@physics.rutgers.edu

[a] BioMaPS Institute, Rutgers University, Piscataway, NJ 08854, USA

[b] Department of Physics and Astronomy, Rutgers University, Piscataway, NJ 08854, USA

[c] Department of Mathematics, Rutgers University, Piscataway, NJ 08854, USA

Abstract

Maintenance of alternative chromatin states through cell divisions pose some fundamental constraints on the dynamics of histone modifications. In this paper, we study the systems biology of epigenetic inheritance by defining and analyzing general classes of mathematical models. We discuss how the number of modification states involved plays an essential role in the stability of epigenetic states. In addition, DNA duplication and the consequent dilution of marked histones act as a large perturbation for a stable state of histone modifications. The requirement that this large perturbation falls into the basin of attraction of the original state sometimes leads to additional constraints on effective models. Two such models, inspired by two different biological systems, are compared in their fulfilling the requirements of multistability and of recovery after DNA duplication. We conclude that in the presence of multiple histone modifications that characterize alternative epigenetic stable states, these requirements are more easily fulfilled.

Keywords

Silencing; Bistability; Epigenetics; Cell cycle; Histone modification

1. Introduction

Epigenetic regulation of multiple heritable cell fates involves transcriptional repression or activation of the expression levels of genes, over possibly many cell cycles, without altering the underlying genetic sequence (Allis et al., 2007). Such regulation is crucial in eukaryotic development where specialized cells with identical genetic information differentiate early on to serve distinct functions. At the heart of one important mechanism of epigenetic control is the accessibility of DNA packaged into higher order structures known as chromatin. The basic unit of such packaging is the nucleosome comprising 146 base pairs of DNA wrapped around a core histone octamer (two each of H2A, H2B, H3 and H4) in $1\frac{3}{4}$ superhelical turns[2] (Lodish et al., 2004). These histones are some of the most evolutionarily conserved proteins known. Covalent post-translational modifications of these histones have been identified to be a critical player in cellular memory. At least seven such modifications (or ‘marks’) are documented and have been studied extensively in recent years; methylation, acetylation,

[*]Corresponding authors at: BioMaPS Institute, Rutgers University, Piscataway, NJ 08854, USA. Tel.: +1732 445 4668; fax: +1732 445 4400.

[1]These authors contributed equally to the work.

[2]Nucleosome may also contain linker histones, e.g. H1 and variants in higher-order structure like the 30nm chromatin fiber.

phosphorylation, ubiquitination, sumoylation and ribosylation. These 'marks' create a favorable binding site for specific regulatory proteins, and thereby play a pivotal role in controlling transcriptional activation and repression, as well as other cellular processes like mitosis/meiosis and DNA repair; for a recent overview see Peterson and Laniel (2004). Another important epigenetic mark is CpG methylation of DNA. In this paper we will be mostly concerned with histone modification, rather than DNA modification, although some of the issues raised may apply to DNA methylation as well.

One of the defining properties of epigenetic phenomena is its stability—the ability of the cell to maintain its epigenetic state through many cell divisions. The marks responsible for the epigenetic effects, be they on DNA itself or on the histones, are bound to get diluted during DNA replication by introducing newly synthesized DNA and histone proteins, indicating that these heritable states must be robust against significant perturbations in the concentration of marks. The aim of this paper is to explore minimal models of epigenetic silencing in order to identify the necessary conditions for stability of chromatin states that correspond to distinct epigenetic phenotypes.

In order to provide a concrete example, let us focus on the tails of histones H3 and H4 which exhibit a number of modifications. Methylation/acetylation of lysines (K) and argininies (R), phosphorylation of serines (S) and threonines (T) on multiple positions on these tails are some examples. Moreover, lysine residues can accept from one to three methylations groups and arginines can be mono- or di-methylated. The majority of these post-translational marks occur on amino-terminal (also called '*N*-terminal tail') and carboxy-terminal (also called '*C*-terminal tail') domains, though examples of modifications within the central domains are beginning to be unraveled. As an example of an *N*-terminal tail modifications, consider the case of H3K9. This lysine can be acetylated or methylated and, as already mentioned, there are three methylated states. There is no detectable H3K9 methylation in *S. Cerevisiae*, however, in *S. Pombe*, *Drosophila* and mammals, methylation of H3K9 have been associated with transcriptional silencing and acetylation has been associated with transcriptional activation (Peterson and Laniel, 2004; Turner, 2002; Strahl and Allis, 2000; Lachner et al., 2003). A combination of such marks defines an epigenetic state, and some of these states are possibly stabilized by histone modifications influencing the presence of one another.

Various enzymes coordinate histone modifications and others bind to modified tails, like chromatin modifying proteins and transcriptional regulatory proteins. From the silenced information regulator (SIR) proteins in budding yeast, regulating repression of gene expression from hidden mating loci and from telomeres (Lodish et al., 2004), to silencing of developmentally important Hox genes in metazoans by the Polycomb group of proteins (Gilbert, 2003), mechanisms of chromatin silencing involve enzymes that can act on more than one nucleosome in its neighborhood (Grewal and Moazed, 2003). This non-locality of action opens the possibility of interesting collective aspects of stability of epigenetic states.

2. A general stochastic model of epigenetic inheritance

We consider a lattice of size L whose sites correspond to nucleosomes ordered along the length of the chromatin. The nucleosome corresponding to site i, has multiple states, corresponding to particular combinations of modifications of a set of side chains that we are interested in. These states are labeled by $s = 1, \ldots, N$. The rates of transition at site i from state s' to state s, namely, $R_{iss'}[s_1, \ldots, s_{i-1}, s', s_{i+1}, \ldots, s_L]$, depends not only on the local state but also on the states of all the neighbors within a range l. In practice, this dependence arises because particular modifications of a site leads to recruitment of particular histone

modifying enzymes that could affect modification rates of the neighboring nucleosomes. Fig. 1 provides a schematic representation the model and its dynamics.

The master equation describing the time evolution of the probability distribution $P[s_1, \ldots, s_L; t]$ is given by

$$\frac{d}{dt}P[s_1,\ldots,s_L;t] = \sum_{i=1}^{L}\sum_{s'}(R_{is_is'}[s_1,\ldots,s_{i-1},s',s_{i+1},\ldots,s_L]\times P[s_1,\ldots,s_{i-1},s',s_{i+1},\ldots,s_L;t] - R_{is's_i}[s_1,\ldots,s_{i-1},s_i,s_{i+1},\ldots,s_L]P[s_1,\ldots,s_{i-} \quad (1)$$

for times between DNA replication. At the point of DNA duplication, existing histones components like H3–H4 octamers and H2A–H2B dimers get distributed with equal probability to the resulting pair of DNA molecules (Sogo et al., 1986; Krude and Knippers, 1991; Gasser et al., 1996). This process retains some memory of the original state. In addition, newly synthesized histones also get deposited. Thus the process of DNA duplication and subsequent reassembly of nucleosomes retain, as well as dilute, the information carried by epigenetic marks.

While considering the result of duplication, we would always track one of the two resulting cells. In this paper, we ignore the variability of histone marks over the cell cycle. We assume that, independently at each site i, there is one half probability of having the parental histones with epigenetic marks and one half probability of it being replaced by a newly synthesized histones where the state of histone modification s comes with probability p_s. The process of de novo assembly of histones can be thought to be independent of existing histone modifications. Therefore, we represent the evolution of the probability distribution from the parental cell to one of its progeny, due to replication and reassembly, as follows:

$$P[s_1,\ldots,s_L;nT+] = \sum_{s'_1,\ldots,s'_L}\prod_{i=1}^{L}\left(\frac{1}{2}\delta_{s_i,s'_i}+\frac{1}{2}p_{s'_i}\right)P[s'_1,\ldots,s'_L;nT-] \quad (2)$$

where $nT+$ and $nT-$ refer to the times just after and just before the n-th round of DNA duplication happening with a time period of T. We assume that DNA duplication happens instantaneously (in reality, fast compared to the time between two duplication events), namely it occurs at times $t = nT$, n being an integer.

We will study, computationally, the stochastic model of epigenetic inheritance formulated above for a particular choice of states and rules of state transitions. However, to gain some insight, it will be useful to carry out a parallel analytical approach which will be described in the next section.

3. Mean-field theory

To solve the master equation analytically for the long time behavior of $P[s_1, \ldots, s_L; t]$ is generally an impossible task. One, therefore, has to resort to some sort of approximation. One such approximation often used successfully in statistical mechanics is the 'mean-field' approximation (Reichl, 1997). In this approach one approximates $P[s_1, \ldots, s_L; t]$ by a factorized form $\Pi_i p_i[s_i; t]$. Using this approximation one derives that the evolution equation for $p_i[s_i; t]$ is going to be

$$\frac{d}{dt}p_i[s_i;t]=\sum_{s'}(\bar{R}_{is_is'}p_i[s';t]-\bar{R}_{is's_i}p_i[s_i;t]) \tag{3}$$

where the definition of the average rates $\bar{R}_{iss'}$ is

$$\bar{R}_{iss'}=\sum_{s_1,\ldots,s_{i-1},s_{i+1},\ldots,s_L}R_{iss'}[s_1,\ldots,s_L]\times p_1[s_1;t]\ldots p_{i-1}[s_{i-1};t]p_{i+1}[s_{i+1},t]\ldots p_L[s_L;t] \tag{4}$$

Notice that these averaged rates $\bar{R}_{iss'}$ are polynomials in $p_i[s; t]$ making Eq. (3) a nonlinear equation.

We also need the equivalent of Eq. (2), capturing the effect of DNA duplication.

$$\begin{aligned}p_i[s_i';nT+]&=\sum_{s_i'}\left(\tfrac{1}{2}\delta_{s_i,s_i'}+\tfrac{1}{2}p_{s_i'}\right)p_i[s_i';nT-]\\&=\frac{p_i[s_i;nT-]+p_{s_i}}{2}\end{aligned} \tag{5}$$

In the mean-field analysis of all the models discussed in this paper, we will ignore the spatial variation of 'marks' and replace them by average concentrations corresponding to an entire region of chromatin, namely $p_i[s_i; t] = p[s_i; t]$. We thereby focus on regions of chromatin with one epigenetic fate and in the spirit of exploring minimal dynamical models, we claim that the study of just few histone modification states can already lead to nontrivial insight about the dynamical system. For example, recent work by one of the authors has addressed one such model of silencing that included spatial structure, leading to predictions about the propagation of silencing, see Sedighi and Sengupta (2003). In this paper we will be concerned with inheritance of 'uniform' states. The equations for the variables $p[s; t]$

$$\frac{d}{dt}p[s;t]=\sum_{s'}(\bar{R}_{ss'}p[s';t]-\bar{R}_{s's}p[s,t]) \tag{6}$$

where $\bar{R}_{ss'} = \bar{R}_{iss'}$, is given by Eq. (3). They are independent of i because the rules of transitions are translation invariant and we ignore boundary effects. The equivalent of Eq. (2), indicating the effect of DNA duplication, in the mean-field context is

$$p[s;nT+]=\frac{p[s;nT-]+p_s}{2} \tag{7}$$

We remind the reader of some well-known aspects of the mean-field approximation commonly used in statistical physics, in order to make the present discussion self-contained. On incorporating recruitment and cooperative behavior multiple neighboring sites of a site influence the probability of the state at that site, therefore, the transition rates are dependent on what happens on neighboring sites. In what sense can these rules of transition be thought as depending solely on the state of histone modification on the site? To answer this, we suppose that the rates $R_{is_is'}[s_1, \ldots, s_{i-1}, s', s_{i+1}, \ldots, s_L]$ depend only on the fraction of sites in a given state in the neighborhood of i within separation l, where $1 \leq l$ (we could still have $l \leq L$ to be physically meaningful). That mean-field theory is applicable, and very often an excellent approximation, can be understood by defining mean-field averaged quantities, i.e., coarse-graining the system. We can group L sites into L/l clusters of l sites each. We redefine the probabilities $p_i[s_i, t]$ of state s_i at site $i \in [1, L]$ by the averaged probability $\bar{p_j}[s, t]$ of state S at any cluster $j \in [1, L/l]$, where formally

$$\overline{p}_j[S,t] \equiv \frac{1}{l}\sum_{i=jl-l+1}^{jl} p_i[s_i,t] \tag{8}$$

Now we can assume that the averaged probabilities are approximately site independent. The approximation turns out, a posteriori, to be justified when the chemical noise in the concentrations of the states is relatively small, and the system is not near a dynamical critical point. The new states S are not binary corresponding to the presence or absence of marks but a discrete spectrum of states that can be approximated by the concentration of marks in a cluster. This mean-field equivalence of the local probability of a binary state at a site to the probability density (or normalized concentration) of states in a 'coarse-grained cluster' is going to be exploited in the rest of the paper implicitly in writing down mean-field differential equations for the dynamics of the system. We will not introduce in the rest of the paper the formal redefinitions of probabilities done above.

4. Two-state model

Abiding by our goal of identifying a minimal model of epigenetic silencing, we outline in this section a two-state model of stable epigenetic marks and observe that without cooperativity one cannot obtain bistability in such models. This is instructive in appreciating the role of multiple heritable histone modifications in stable epigenetic states.

Here the epigenetic state s could be just the presence (A) or absence of a mark (U), and therefore the probabilities are, with notational simplification, $p_j[A, t] = a_j(t)$ and $p_j[U, t] = u_j(t) = 1 - a_j(t)$, where, for example, $a_j(t)$ could be the probability of finding the acetylation mark A on H4K16 on a nucleosome of the chromatin of budding yeast *S. Cerevisiae* and $u_j(t)$ of finding that lysine unmodified (deacetylated). The rate constant for an acetylated mark to be deacetylated owing to histone deacetylase (HDAC) activity and natural degradation is given by γ_A, i.e., $R_{jUA} = \gamma_A$. To include the effect of recruitment of acetylases by acetylated marks we define a rate constant of recruitment α_A. We obtain the mean-field expressions for this rate as follows:

$$\overline{R}_{jAU}=\frac{\alpha_A}{2}\{a_{j+1}(t)+a_{j-1}(t)\} \tag{9}$$

$$\overline{R}_{AU} \approx \alpha_A a(t) \tag{10}$$

Similarly, we also include the effect of recruitment of deacetylases by unmodified sites, for example, SIR2 protein complex is known to have deacetylation activity and is recruited by deacetylated sites, and the rate constant for this process is denoted by η_A. The constant rate of acetylation of an deacetylated mark is denoted by χ_A. With these definitions, we obtain the equation for the rate of acetylation,

$$\frac{da(t)}{dt}=(1-a(t))(\chi_A+\alpha_A a(t))-(\gamma_A+\eta_A(1-a(t)))a(t) \tag{11}$$

In the spirit of this paper, this is the simplest model one can examine. This model has only one stable state given by

$$a^*=\frac{1}{2\bar{\alpha}_A}(\bar{\alpha}_A-\gamma_A-\chi_A+\sqrt{4\bar{\alpha}_A\chi_A+(\bar{\alpha}_A-\gamma_A-\chi_A)^2}) \tag{12}$$

where $\bar{\alpha}_A \equiv \alpha_A - \eta_A$. This solution goes to one for vanishing rate of degradation γ_A. This behavior is insufficient as far as epigenetics is concerned—the model fails to produce bistability even in the absence of a cell cycle. Including DNA duplication in the model will not produce multiple dynamical attractors. This very simple analysis leads us to conclude that cooperativity (of histone modifications) is necessary in a two-state model to attain bistability, as we shall soon present. In the context of the specific example of silencing in *S. Cerevisiae* (Kurdistani and Grunstein, 2003), SIR complex of proteins bind cooperatively at a deacetylated site; see Sedighi and Sengupta (2003) for modeling of this system.

Thus, if we allow the deacetylated and acetylated sites in the above model to recruit enzymes cooperatively to deacetylate and acetylate neighboring sites, respectively, then the above model is modified to

$$\frac{da(t)}{dt}=(1-a(t))\{\chi_A+\alpha_A a^n(t)\}-\{\gamma_A+\eta_A(1-a(t))^m\}a(t) \tag{13}$$

where the degree of cooperative acetylation is n and the degree of cooperative deacetylation is m. Assume that the basal rates are very small—χ_A and γ_A can be ignored to the lowest order approximation. For the simplest case of cooperative behavior

$$\left\{a=1, a=0, a=\frac{\eta_A}{\alpha_A+\eta_A}\right\} \tag{14}$$

where the first two are stable fixed points, showing explicitly that both a high mark and a low mark state is stabilized by cooperative effects. More generally, call $f(a)$ the RHS of Eq. (13) with $n = 2$, $f(a)$ will have three zeros, $a_1<a_2<a_3$ in the interval [0, 1]. The scenario relevant to us is when a_1 and a_3 is stable and is separated by unstable a_2.

Any initial states with $a(0)<a_2$ will eventually be attracted to a_1 and any initial state with $a(0)>a_2$ will eventually be attracted to a_3. Now suppose that the cell undergoes mitosis with a typical cell-cycle period of T. For simplicity, assume that mitosis exactly halves the concentration of marks on chromatin. If $a_2 \geq a_3/2$ then, for cell-cycle time T considerably larger than the timescale of histone modification rates, only one fixed point will be stable to cell-cycle perturbations over many cell-cycles, and this fixed point will be approximately a_1. This can be understood as follows. Even when the system starts close to a_3 (corresponding to high concentration of marks), the concentration of marks after mitosis will be less than a_2 and, therefore will be in the basin of attraction of the stable fixed point a_1 (low concentration of marks). However, for $a_2<a_3/2$ and T fulfilling the same conditioned stated earlier, two fixed point will be stable to such cell-cycle perturbations. This condition implies that $\eta_A<\alpha_A$ for stability when χ_A and γ_A are negligible. For fairly explicit expressions for T in terms of $f(a)$ and restrictions on the parameters entering $f(a)$ and T obtained from requiring stability, see Appendix A.

Going beyond mean-field theory, we use simulations to explore the tolerance of the system to changes in the rate parameters and its stability against cell-cycle perturbation and chemical noise. Details of the simulation are provided in Appendix C.

Comparison of the simulation of this model against mean-field theory is shown in Fig. 2. The most important conclusions from this study are the following. We have already observed that even at the mean-field level, the requirement of stability against cell-cycle perturbations impose constraints on the rate parameters. In particular, the constraint $\eta_A<\alpha_A$ implies that the cooperative conversion of U's into A's is stronger than the cooperative conversion of A's into U's. Therefore, even when the rates of γ_A and χ_A (i.e., the rates for spontaneous creation and decay of A) are small, which it should be in order for the epigenetic marks to be stable within a cell-cycle period, the fluctuations in U turning into A are magnified compared to the fluctuation in A turning into U. As an example of this 'instability' of the system for a reasonable choice of values for the rate parameter, see Fig. 3. The concentration $a(t)$ is plotted against time for two initial states, $a(t_0) = 0$ and 1. In all these studies, we always consider cell-cycle period to be much larger than the typical relaxation times to reach a stable state. Nevertheless, spontaneous fluctuations may flip a low A state to a high A state eventually, often within a few cell-cycles. This phenomena is quite striking when compared to the behavior of the three-state model we introduce in the next section. To anticipate our results, we observe that a three-state model is more stable in the above sense, and we thereby postulate that presence of multiple epigenetic marks is a design criterion for epigenetic stability.

An alternative way to think about this phenomenon is as follows. Let us ask ourselves how can we go beyond mean-field theory. Even if the uniform solution with a nearly zero is stable in mean-field theory, there is always a non zero probability of nucleating a cluster of few A sites among all the U's. This configuration has two boundaries between the all A phase and the all U phase. The condition $\eta_A<\alpha_A$, a consequence of the constraint imposed by the states surviving through cell cycle, implies that, on the average the boundary would propagate into the all U region. This is the phenomenon of front propagation between two stable states (Aronson and Weinberger, 1975; Cross and Hohenberg, 1993). The linear growth of acetylation shown in Fig. 2 is the consequence of such a constant front velocity.

The only way we could make the deacetylated state survive for many rounds of cell cycle is by having the probability of the initial nucleation lowered. This indeed happens in models where the range of interaction l is large, as we have seen from our simulation of related models (data not shown). The nucleation probability is also low for the three-state model as we will argue, later.

5. Three-state model

Having explored a two-state mean-field model and its limitations in the previous section, we now study a simple three-state mean-field model of histone modification, originally proposed in the context of silencing in fission yeast *S. pombe* (Dodd et al., 2007), where the states are unmodified (*U*), methylated (*M*) and acetylated (*A*). This model is a simple example from a class of models where we will prove that bistability is a result of the presence of recruitment of multiple marks. For the sake of clarity, a concrete example of a three-state model could be the acetylation and methylation marks on H3K9. We belabor the spirit of this analysis—we are not pretending that these modifications on the histone are independent of other modifications, or that a high acetylation or high methylation on any histone tail protein leads to identical functional outcomes, we are, instead, interested in clarifying the distinctions in stability of epigenetic inheritance obtained in the presence of multiple marks. The stable fixed points we analyze could as well be combination of various histone modifications.

Coming back to the example, a methylated site recruits further methylation of neighboring nucleosomes and an acetylated site similarly recruits further acetylation. The epigenetic states *s* are high methylation, high acetylation and unmodified site. Therefore, we denote the mean-field probabilities as $p[M;\, t] = m(t)$, $p[U;\, t] = u(t)$ and $p[A;\, t] = a(t)$. These probabilities obey the conservation law $m(t) + u(t) + a(t) = 1$. Let α_M be the net (recruited) enzymatic activity of histone methyltransferase (HMT) which converts *U* to *M* and of histone demethylase (HDM) which converts *M* to *U*. Similarly, let α_A be the net (recruited) enzymatic activity of histone acetyltransferase (HAT) which converts *U* to *A* and HDAC which converts *A* to *U*. We also include recruited conversion of *A* to *U* in the presence of *M* parametrized by the enzymatic activity β_M, and *M* to *U* in the presence of *A* parametrized by β_A. The kinetic equations for the concentrations are given by

$$\frac{dm(t)}{dt} = \alpha_M u(t) m(t) - \beta_M m(t) a(t) \tag{15}$$

$$\frac{da(t)}{dt} = \alpha_A u(t) a(t) - \beta_A a(t) m(t) \tag{16}$$

One should include basal rates of conversion of *U* to *M* and *U* to *A* given by rate constants χ_M and χ_A, natural degradation and conversion rates of *M* to *U* and *A* to *U* given by rate constants γ_M and γ_A, and we will do so shortly. We can further embellish this minimal model to suit other observed features like protein regulations, intermediate states like di- or mono-methylation etc., but the key aspect of bistability is already captured at this level of sophistication, and we think it is instructive to present that without complicating the model. The fixed points of the above equations are determined by the simultaneous roots of the quadratic polynomial, obtained by setting the LHS of Eqs. (15) and (16) to zero. They are given by

$$\{a^*=1, m^*=0\}, \{a^*=0, m^*=1\}, \{a^*=0, m^*=0\},$$
$$\left\{a^*=\frac{\alpha_M\beta_A}{\alpha_A\beta_M+(\alpha_M+\beta_M)\beta_A}, m^*=\frac{\alpha_A\beta_M}{\alpha_A\beta_M+(\alpha_M+\beta_M)\beta_A}\right\}$$

It can be easily checked that the first two fixed points are stable, the third fixed point is an unstable saddle point and the fourth point is unstable. It is not hard to convince oneself that if one includes small basal rates the stability of the model remains unaffected, and we come back to this later.

This simple level of modeling may already be quite relevant. We observe that in the absence of active chromatin remodeling processes which may dictate basal rates for conversion and degradation of marks, recruitment alone ensures that methylated and acetylated states are quite robust against mitotic perturbations. During mitosis, the parental nucleosomes with marks are distributed randomly to daughter chromatins, however, newly synthesized nucleosomes are modified by recruitment from neighbors, restoring the original state. Cooperativity is not necessary. One can argue that the prevalence of multiple modifications of histones, instead of just unmodified and uniquely modified histones (a two-state scenario), is owing to this efficient robustness achieved through multiple states. The reason for this increased stability lies in the higher dimensionality of the space of configurations and the fact that multiple transitions (say, $M \rightarrow U \rightarrow M$, at more than one neighboring sites) need to take place before one nucleates the other stable phase.

For the sake of completeness, we now analyze the model by including basal rates for conversion and degradation. The new equations are

$$\frac{dm(t)}{dt}=\alpha_M u(t)m(t) - \beta_M m(t)a(t)+\chi_M u(t) - \gamma_M m(t) \tag{17}$$

$$\frac{da(t)}{dt}=\alpha_A u(t)a(t) - \beta_A a(t)m(t)+\chi_A u(t) - \gamma_A a(t) \tag{18}$$

A plot of the flow lines when high *A* and high *M* states are stable is shown in Fig. 4. Points are evenly distributed on a grid and allowed to evolve for a fixed time in generating the flow lines numerically. The hue of the plotted lines is changed linearly in time. A similar plot for the scenario when the high *A* and high *M* states are unstable as shown in Fig. 5. This is the case when the degradation rates are too high. Stability analysis around the fixed points of these equations is relegated to Appendix B. The lattice-averaged concentration of mark $a(t)$ as a function of time is plotted in Fig. 6.

6. Conclusion

We have formulated a mathematical model of inheritance of epigenetic silencing and showed how we have two routes to producing stable epigenetic states: one via cooperativity of silencing factor recruitment and the other via the presence of multiple marks, where there are barrier states between an active and a repressed states. We also found that multiple marks allow the cell higher stability to cell-cycle perturbations, in comparison to a single mark system. We believe that the robustness of these models to cell-cycle perturbation may be a reason why multiple histone modifications are observed frequently in epigenetic design. We note, however, that at a fundamental level these two are not entirely distinct routes. The

presence of intermediate states naturally lead to cooperative effects when each of the intermediate states recruit enzymes for further modification. Moreover, protein complexes that induce further enzymatic activity often possess domains that simultaneously recognize histone modifications at adjacent sites. This is thought to be the case with SIR protein complex and also for the polycomb silencing mechanism. Effective cooperativity can emerge on eliminating transient intermediate states in models with first order rates.

We have phrased the mean-field theory in terms of coarse-grained quantities like the fraction of sites with a particular mark in a cluster. For those readers familiar with statistical physics, a natural question is how does the effective model change if we continue the coarse-graining to larger length scales. In other words: one could ask how the model 'renormalizes' under iterative blocking transformations (Reichl, 1997). In practice, setting up a reasonable scheme for doing such block transformation may be difficult. However, we could make some educated guesses about what would happen. In absence of any conservation law, there is no obvious reason why this system should not have a finite (although long) correlation length in space and, similarly, a finite correlation time. The system would not have genuinely multiple phases. All these effects, which are missed by mean-field theory, would, in principle, show up in renormalization group transformations. We had already mentioned how the system could get out of one of the phases, by nucleation of the other phase, and showed some numerical evidence that, in fact, it does so. Such nucleation gives rise to domain boundaries, which are responsible for finite correlation length in the system. Technically, therefore, the system becomes very weakly coupled if we coarse-grain to blocks with size larger than the correlation length.

Having said that, in the biological context, the domains usually incorporate a few hundred nucleosomes and epigenetic states are stable for somewhere between 10 and 100 cell cycles. It is enough for the model to produce correlation lengths and correlation times in those ranges. Mean-field theory gives us a hint when such correlated states appear. However, in this approximation, long, but finite, lifetimes become infinite.

As we saw, for both states to be long-lived, we need suppression of the probability of spontaneous nucleation of the more stable state (as measured by average front velocity helping to spread the state). This can be achieved either by having a more complex model which requires multiple marks to occur before nucleation happens, or by having a long range model where many sites have to have unlikely changes before the nucleation is complete.

In practice, for the systems biology of silencing, the possibility of more complex models is worth serious consideration, especially when there is no obvious mechanism of cooperativity and there appears to be a plethora of histone marks that are involved in the process. In addition, these models have different degree of robustness to variation of conditions from cell to cell. Many of the parameters in the model are not just chemical reaction rates but also depend upon abundances of certain proteins in the cell. For example, the effect of the neighbors is often through recruitment of histone modifying enzymes not explicitly modeled. Variation in the abundance of those enzymes would change the effective parameter from cell to cell. On the other hand, if the biochemistry dictates that the basal modification rates are very small, say compared to modification due to recruited enzymes, the basal reactions are unlikely to become significant player in any of the cells. If one neglects the basal rates, the two-state model has an additional constraint on the nonzero parameters, in addition to constraints of multistability, whereas the three-state model does not have such an additional condition. As a result, we expect the functionality of the second model to be more immune to cellular variability.

The interaction between cell cycle and epigenetic silencing is a rich subject in biology. We have only focused on one aspect of it in these models, namely, the recovery of the epigenetic information after the dilution caused by DNA duplication, and ignored other phenomena like cell cycle dependent histone modifications. However, even within our simplest setup, different classes of models give rise to interesting differences in performance. Exploring such models in combination with experiment designed to test qualitative predictions valid for a broad class of models is the way to gain insight into the nature of epigenetic inheritance.

Acknowledgments

We acknowledge useful discussions with Adel Dayarian and Mohammad Sedighi. Two of the authors (A.M.S. and S.M.) were partially supported by an NHGRI Grant R01 HG03470-02. J.L.L.'s work was partially supported by NSF Grant DMR-0802120 and AFOSR Grant AF-FA-9550-04-4-22910.

References

Allis, CD.; Jenuwein, T.; Reinberg, D. Epigenetics. Cold Spring Harbor Laboratory Press; Cold Spring Harbor, NY: 2007.

Aronson, D.; Weinberger, H. Non-linear diffusion in population genetics and nerve pulse propagation. In: Goldstein, J., editor. Partial Differential Equations and Related Topics. Springer Lecture Notes in Mathematics. Vol. 446. Springer, NY; 1975. p. 5-49.

Cross MC, Hohenberg PC. Pattern formation outside of equilibrium. Reviews of Modern Physics 1993;65 (3 part II):851–1112.

Dodd IB, Micheelsen MA, Sneppen K, Thon G. Theoretical analysis of epigenetic cell memory by nucleosome modification. Cell 2007;129:813–822. [PubMed: 17512413]

Gasser R, Koller T, Sogo J. The stability of nucleosomes at the replication fork. Journal of Molecular Biology 1996;258 (2):224–239. [PubMed: 8627621]

Gilbert, S. Developmental Biology. Sinauer; Sunderland, MA: 2003.

Grewal SIS, Moazed D. Heterochromatin and epigenetic control of gene expression. Science 2003;301:798–802. [PubMed: 12907790]

Krude T, Knippers R. Transfer of nucleosomes from parental to replicated chromatin. Molecular And Cellular Biology 1991;11 (12):6257–6267. [PubMed: 1658628]

Kurdistani SK, Grunstein M. Histone acetylation and deacetylation in yeast. Nature Reviews. Molecular Cell Biology 2003;4:276–284. [PubMed: 12671650]

Lachner M, O'Sullivan RJ, Jenuwein T. An epigenetic road map for histone lysine methylation. Journal of Cell Science 2003;116:2117–2124. [PubMed: 12730288]

Lodish, H., et al. Molecular Cell Biology. WH Freeman; New York, NY: 2004.

Peterson C, Laniel M. Histones and histone modifications. Current Biology 2004;14 (14):546–551.

Reichl, LE. A Modern Course in Statistical Physics. 2. Wiley; New York, NY: 1997.

Sedighi M, Sengupta AM. Epigenetic chromatin silencing: bistability and front propagation. Physical Biology 2003;4:246–255. [PubMed: 17991991]

Sogo J, Stahl H, Koller T, Knippers R. Structure of replicating simian virus 40 minichromosomes. The replication fork, core histone segregation and terminal structures. Journal of Molecular Biology 1986;189:189–204. [PubMed: 3023620]

Strahl BD, Allis D. The language of covalent histone modifications. Nature 2000;403:41–45. [PubMed: 10638745]

Turner B. Cellular memory and the histone code. Cell 2002;111 (3):285–291. [PubMed: 12419240]

Appendix A. General case for two-state model

In the general case for the two-state model's mean-field equation, we may formally define $f(a)$ as

$$\frac{da(t)}{dt}=Q(a)\Pi_i(a_i-a(t))=f(a) \tag{19}$$

where $0\le a_1<a_2<a_3\cdots<a_{2k+1}\le 1$ and $Q(a)>0$ for $0\le a\le 1$. We focus on the scenario when there are odd number of stationary points because we want $f(0)\ge 0$, $f(1)\le 0$ for our purpose. The odd zeros of $f(a)$, i.e., $a_1, a_3, \ldots, a_{2k+1}$ will be linearly stable fixed points while the even number zeros will be unstable fixed points.

If we now consider the effect of mitosis—the halving of the fraction of occupied sites—then the new fixed points stable to mitosis a_i^* corresponding to the original stable fixed points a_j are such that $a_0=0<a_1^*\le a_1/2,\ldots.<a_{2j+1}^*\le a_{2j+1}/2,\ldots$.

Let T_i be the period between mitosis in which the fraction of marked sites will increase from a_j^* to $2a_j^*$ during a cell cycle. Setting $Q(a) = 1$ and integrating Eq. (19), we get

$$T_i=\int_{a_i^*}^{2a_i^*}\frac{ds}{\Pi(a_i-s)}=\sum_{j=1}^{2k+1}B_j\log\frac{a_j-a_i^*}{a_j-2a_i^*} \tag{20}$$

where the B_j's can be computed in terms of the a_i's. The allowed range of values of the stable fixed point a_i^* is a function of T and the rate parameters defining the dynamics of histone modifications, encoded in B_j's and a_j's. One can easily extend this analysis to include more general $Q(a)$.

Appendix B. Linear stability analysis for three-state model

The expressions for the fixed points of the set of Eqs. (17) and (18) are somewhat more involved than that of Eqs. (15) and (16). For the sake of clarity, we only present the results for the situation when $\alpha_A\approx\alpha_M:=\alpha$, $\beta_A\approx\beta_M:=\beta$, $\gamma_A\approx\gamma_M:=\gamma$ and $\chi_A\approx\chi_M:=\chi$. The essential features of the model are captured in this approximation and the algebra simplifies considerably. (The analysis can be extended easily to the asymmetric case by numerical methods.) This gives the following pairs of fixed points,

$$\begin{gathered}\left\{m_1^*:=\frac{\alpha\beta-\beta\gamma+\sqrt{(\alpha\beta-\beta\gamma)^2-4\alpha\beta\gamma\chi}}{2\alpha\beta}\right\}\\ \left\{a_1^*:=\frac{\alpha\beta-\beta\gamma-\sqrt{(\alpha\beta-\beta\gamma)^2-4\alpha\beta\gamma\chi}}{2\alpha\beta}\right\}\\ \left\{m_2^*=a_1^*,\ a_2^*=m_1^*\right\}\\ \left\{m_3^*:=\frac{\alpha-\gamma-2\chi-\sqrt{4\chi(2\alpha+\beta)+(\alpha-\gamma-2\chi)^2}}{2\alpha(2\alpha+\beta)},\ a_3^*=m_3^*\right\}\\ \left\{m_4^*:=\frac{\alpha-\gamma-2\chi+\sqrt{4\chi(2\alpha+\beta)+(\alpha-\gamma-2\chi)^2}}{2\alpha(2\alpha+\beta)},\ a_4^*=m_4^*\right\}\end{gathered} \tag{21}$$

Note that for $\gamma=\chi=0$ the solutions map onto the solutions to Eqs. (15) and (16), as they should.

We only analyze the stability of fixed points of Eqs. (17) and (18) for small basal rates χ and γ. We know that for vanishing γ and χ the pair of roots $\{m_1^*, a_1^*\}$ and $\{m_2^*, a_2^*\}$ are stable. Around the $\{m_1^*, a_1^*\}$ fixed point the matrix that determines the stability is

$$\begin{pmatrix} -\alpha+\gamma-\chi-\frac{\gamma\chi}{\alpha}-\frac{\gamma\chi}{\beta} & -\alpha-\beta+\gamma-\chi+\frac{\gamma\chi}{\beta}+\frac{\gamma(\beta+\chi)}{\alpha} \\ -\frac{\chi(\beta\gamma+\alpha(\beta+\gamma))}{\alpha\beta} & \frac{\beta\gamma(\beta+\chi)-\alpha(\beta^2+\beta\chi+\chi\gamma)}{\alpha\beta} \end{pmatrix} \tag{22}$$

where the only terms up to first order in γ and χ have been retained. The matrix around the second fixed point $\{m_2^*, a_2^*\}$ is obtained by swapping the rows of the above matrix. The eigenvalues of the above matrix are determined to be

$$\begin{aligned} E_1 &:= -(\alpha+\beta+|\alpha-\beta|)\left(\tfrac{1}{2}+\tfrac{\chi}{|\alpha-\beta|}-\tfrac{\gamma}{2\alpha}\right)-\tfrac{4\gamma\chi}{|\alpha-\beta|} \\ E_2 &:= -(\alpha+\beta-|\alpha-\beta|)\left(\tfrac{1}{2}-\tfrac{\gamma}{2\alpha}-\tfrac{\chi}{|\alpha-\beta|}\right)-\chi\left(1-\tfrac{4\gamma}{|\alpha-\beta|}\right) \end{aligned} \tag{23}$$

These eigenvalues are negative for γ and χ small compared to α and β, which shows linear stability of the first two fixed points. Though the above expression was obtained by a small γ and small χ expansion and therefore cannot be applied to determine the exact relationship between the parameters for which the fixed points change stability, a rough estimate can be made. Even when $\alpha, \beta \gg \gamma, \chi$, for vanishing γ, when $\chi > |\alpha - \beta|/2$ the second eigenvalue changes to positive.

Appendix C. Simulation details

We simulate a cooperative two-state model (with cooperativity index $n = m = 2$) by directly implementing the master equation for reactions on an one-dimensional circular lattice. The lattice size in this study was 500. Each site i has a mark A or U. In the spirit of Monte Carlo (MC) algorithm, at each time-step a random site is chosen. In implementing cooperativity at the level of elemental reactions, there are many possible choices that are consistent with the mean-field equations for the two-state model. This freedom is present because the number of neighbors of a particular site that influence cooperative behavior and the rules by which they do so, is undertermined at the mean-field level owing to the coarse-graining involved in arriving there. In our implementation, we simply assign local transition probabilities proportional to the local concentration of a mark in the nearest neighborhood. We use

$$\begin{aligned} U_i+A_{i+1}+A_{i-1} &\to A_i+A_{i+1}+A_{i-1};\ \text{rate}\ \alpha_A\ \text{and prob.}1 \\ U_i+A_{i\pm1} &\to A_i+A_{i\pm1};\ \text{rate}\ \alpha_A\ \text{and each with prob.}\tfrac{1}{2} \\ A_i+U_{i+1}+U_{i-1} &\to U_i+U_{i+1}+U_{i-1};\ \text{rate}\ \eta_A\ \text{and prob.}1 \\ A_i+U_{i\pm1} &\to U_i+U_{i\pm1};\ \text{rate}\ \eta_A\ \text{and each with prob.}\tfrac{1}{2} \\ A_i &\to U_i;\ \text{rate}\ \gamma_A \\ U_i &\to A_i;\ \text{rate}\ \chi_A \end{aligned} \tag{24}$$

Comparison of the dynamics of the system under other possible reaction rules that would nevertheless lead to the same mean-field equation is beyond the scope of this study, but we emphasize that they can indeed be quite distinct, as often encountered in non-equilibrium statistical models. Nevertheless, we have checked that the dynamics under other rules lead to the same conclusions made in this paper about the two-state-cooperative model.

In order to compare with the mean-field estimates and establish its validity, we solve the system of coupled nonlinear ODEs given by Eq. (17) numerically. Fitting the results of simulation require fixing a time-scale because in the simulation only relative rates feature. This is because at each MC step, one reaction is always attempted, no matter what the absolute rates are. This fitting time-scale can be estimated as follows. The time corresponding to a MC step is, to a good approximation, determined by the typical time-scale for the fastest reaction to occur when attempts at the fastest reaction is most often successful. In our case, the rates for cooperative reactions are much bigger than the spontaneous creation and decay rates, and therefore the latter can be ignored for this estimate. Moreover, the success rate for both of the cooperative reactions are high for the system close to a random state of *U*'s and *A*'s distributed with probability one-half. In our simulation, this is the state immediately after mitosis. Now, the mean-field equation for vanishing χ_A and γ_A, expanded around $a(t)=\frac{1}{2}$, in terms of $\Delta a(t)=a(t)-\frac{1}{2}$ is

$$\frac{d\Delta a(t)}{dt}=\frac{\alpha_A-\eta_A}{8}+\frac{1}{4}(\alpha_A+\eta_A)\Delta a(t) \tag{25}$$

whose solution, expanded for small *t* is

$$\Delta a(t)\xrightarrow{t\approx 0}\frac{(\alpha_A-\eta_A)t}{8} \tag{26}$$

Now, in the simulation, we have scaled all rates by the sum of rates so that they lie within the unit interval. Note that because $a(t)$ is the concentration, for it to change appreciably all reactions at all sites must have been attempted at least once, therefore, a crude estimate of the time-scale fitting parameter is $\delta t = 8L(\alpha_A + \eta_A)/(\alpha_A - \eta_A)$, where L is the number of sites in the lattice. In all the plots our sampling time for collecting data is L MC steps, therefore, the factor of L is cancelled in this unit. This crude estimate of the time-scale fitting parameter produces a pretty good fit, see Fig. 2. For this plot the chosen rates are, $\alpha_A = 5$, $\eta_A = 2$, $\gamma_A = 0.01$, $\chi_A = 0.01$ and the fitting time-scale is $\delta t = 56/3$.

The simulation of the three-state model is similar to above. The marks at site *i* are instead, *A* or *U* or *M*. The lattice has 500 sites, as before. At each time-step a random site is chosen and one of the following reactions are randomly attempted with a probability proportional to their rate constants:

$$\begin{gathered}U_i+A_{i\pm1}\rightarrow A_i+A_{i\pm1};\ \text{rate}\,\alpha_A\\ U_i+M_{i\pm1}\rightarrow M_i+M_{i\pm1};\ \text{rate}\,\alpha_M\\ M_i+A_{i\pm1}\rightarrow U_i+A_{i\pm1};\ \text{rate}\,\beta_A\\ A_i+M_{i\pm1}\rightarrow U_i+M_{i\pm1};\ \text{rate}\,\beta_M\\ A_i\rightarrow U_i;\ \text{rate}\,\gamma_A,\ \ M_i\rightarrow U_i;\ \text{rate}\,\gamma_M\\ U_i\rightarrow A_i;\ \text{rate}\,\chi_A,\ \ U_i\rightarrow M_i;\ \text{rate}\,\chi_M\end{gathered} \tag{27}$$

We introduce the effect of mitosis as follow. At a regular time-interval we replace each *A* or *M* mark on the lattice by *U* with a probability $\frac{1}{2}$. We ignore p_s, see Eq. (2).

Comparison with mean-field equations is done as before. The chosen rates are, $\alpha_A = \alpha_M = 5$, $\beta_A = \beta_M = 3$, $\gamma_A = \gamma_M = 0.1$, $\chi_A = \chi_M = 0.01$, and the time scaling is $\delta t = 16$, see Fig. 6.

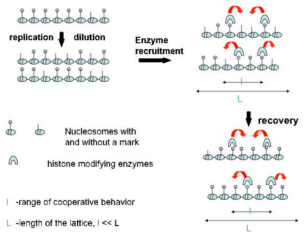

Fig. 1.

A model for inheritance of epigenetic chromatin modification marks. The dilution of marks resulting from replication is remedied by the activity of the histone modifying enzymes recruited by the surviving marks.

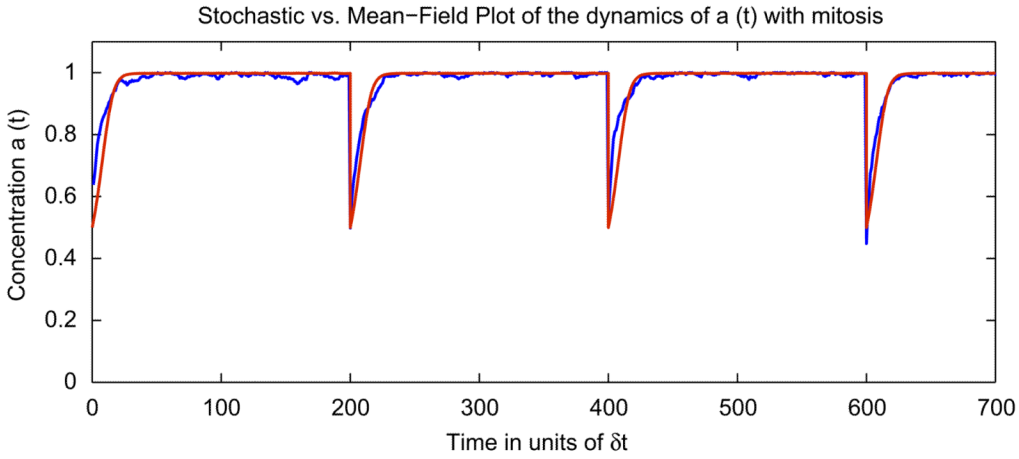

Fig. 2.

Two state model's stochastic simulation, averaged concentration $a(t)$ and mean-field ODE solution fit. Values of parameters: $\alpha_A = 5$; $\eta_A = 2.5$; $\gamma_A = 0.1$; $\chi_A = 0.01$. For the ODE fit, the fitting time-scale is $\delta t = 56/3$.

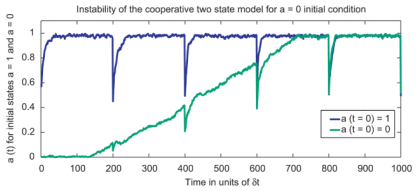

Fig. 3.

Two state model's stochastic simulation, averaged concentration $a(t)$ starting from initial states $a(t = 0) = 1$ and $a(t = 0) = 0$. Values of parameters: $\alpha_A = 5$; $\eta_A = 2$; $\gamma_A = 0.1$; $\chi_A = 0.01$. Though mean-field theory would predict stability, fluctuations compromise it.

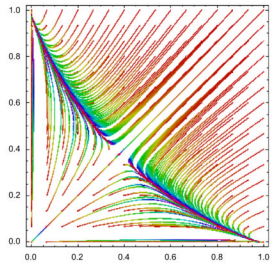

Fig. 4.

Three-state model's phase flow with high *A* and high *M* stable, *x*-axis is $m(t)$ and *y*-axis is $a(t)$. Values of parameters used: $\alpha_A = \alpha_M = 5$; $\beta_A = \beta_M = 3$; $\gamma_A = \gamma_M = 0.1$; $\chi_A = \chi_M = 0.01$.

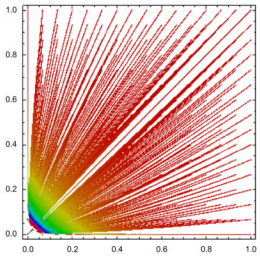

Fig. 5.
Three-state model's phase flow with U stable, x-axis is $m(t)$ and y-axis is $a(t)$. Values of parameters used: $\alpha_A = \alpha_M = 5$; $\beta_A = \beta_M = 3$; $\gamma_A = \gamma_M = 5$; $\chi_A = \chi_M = 0.01$.

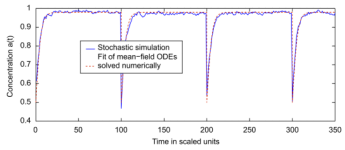

Fig. 6.

Three-state model's stochastic simulation, averaged concentration $a(t)$ and mean-field ODE solution fit. Values of parameters: $\alpha_A = \alpha_M = 5$; $\beta_A = \beta_M = 3$; $\gamma_A = \gamma_M = 0.1$; $\chi_A = \chi_M = 0.01$. For the ODE fit, the fitting time-scale is $\delta t = 15.5$.